Proceedings of CONF-FMCE 2025 Symposium: AI and Machine Learning Applications in Infrastructure Engineering
DOI: 10.54254/2755-2721/2025.MH25948

Aerodynamic Characteristics of NACA2412 and NACA4412 at Low Reynolds Number Numerical Simulation

Jinshi Li

Department of Mechanical and Electronic Engineering, Central South University, Changsha, China
4205220102@csu.edu.cn

Abstract. The aerodynamic performance of airfoils cannot only optimize the lift and drag control of the aircraft to improve the overall performance of the aircraft but also can provide technical support for new concept airfoils, such as bionic airfoil optimization, adaptive deformation wings. However, due to the long cycle of experimental research and the inability to quickly iterate, there are few systematic comparative analyses of such airfoils. Therefore, this paper primarily investigates the two-dimensional aerodynamic characteristics of NACA2412 and NACA4412 at various angles of attack at a Reynolds number of 2.2 × 10^6. ANSYS Fluent was used for geometric modelling and grid division, and the simulation calculation was carried out by using the K-ω SST model and pressure-based solver. The simulation results show that NACA4412 can produce a larger lift coefficient in the range of 0° -12° of the angle of attack. The stall angle of NACA2412 is 16 °, and the stall curve is gentle, while the stall angle of NACA4412 is 13°, and the curve after the stall is steep. Through the systematic comparative analysis of the aerodynamic characteristics of both, it can provide a reference for the subsequent airfoil design and optimization.

Keywords: NACA2412, NACA4412, CFD

1. Introduction

An airfoil is a two-dimensional cross-section of a wing or other aerodynamic surface, and its shape determines the relationship between lift and drag and the wing's angle of attack, thereby determining the aircraft's aerodynamic performance. Proper airfoil selection can significantly enhance lift, reduce drag, delay stall, and mitigate the effects of turbulence, making it a fundamental aspect of aircraft design.

The aerodynamic characteristics of the above airfoils are investigated under various flight conditions. At present, a large number of researchers have studied the above airfoils separately [1]. Pritam Saha et al. investigated the aerodynamic characteristics of NACA2412 at different angles of attack under low Reynolds number conditions, and the results showed that NACA2412 was able to produce good lift at 0–4° attack angles [2]. Chen Zhe et al. took the NACA4412 airfoil as an example, compared the commonly used airfoil lift and drag coefficient calculation methods, and concluded that XFOIL software is fast and inaccurate, while the 2D RANS method based on Fluent is accurate and time-consuming. Yan Wenhui et al. used three kinds of turbulence models, Spalart-Allmaras (S-A), SSTk-ω, Gao-Yong, to numerically calculate the low speed flow around the

DOI: 10.54254/2755-2721/2025.MH25948

NACA4 412 airfoil, and the SSTk-ω model has the best flow detail and lift coefficient calculation, and the Gao-Yong model has the most accurate calculation of the airfoil average velocity profile and Reynolds shear stress distribution [3].

Airfoil design involves not just selecting a geometric shape but also integrating aerodynamic performance considerations for aircraft. Aerodynamic characteristics like lift coefficient, drag coefficient, and stall behavior significantly impact aircraft performance during flight. Comparative research on different airfoils, combining numerical simulations with experimental methods, provides more accurate data for design and optimization. The rapid advancement of computational fluid dynamics (CFD) enables detailed numerical analysis of airfoil aerodynamics, allowing for comprehensive performance evaluation in the design phase. However, there is a lack of comparative studies that fully reveal how airfoil geometric parameters influence aircraft aerodynamics.

In this paper, the aerodynamic characteristics of NACA2412 and NACA4412 are compared based on ANSYS Fluent fluid simulation software, and the aerodynamic characteristics in different attack angles under low Reynolds number are analyzed. Through the analysis of the aerodynamic coefficients and contour diagrams of NACA2412 and NACA4412, the differences in lift characteristics, drag control, and stall characteristics caused by the different cambers of the two airfoils are illustrated. This can not only provide guidance for the design stage of different types of existing aircraft, but also provide a reference for the development and design of new airfoils.

2. Numerical model

2.1. Geometry model and computational domain

In this paper, NACA2412 and NACA4412 are selected as the research objects to simulate the two-dimensional aerodynamic characteristics. The geometric model used for CFD simulation is created by importing the airfoil geometric coordinates into SpaceClaim. The two-dimensional geometric models of NACA2412 and NACA4412 are shown in Figure 1. Figure 2 shows the calculation domain range used for simulation, which is 15 times the chord length.

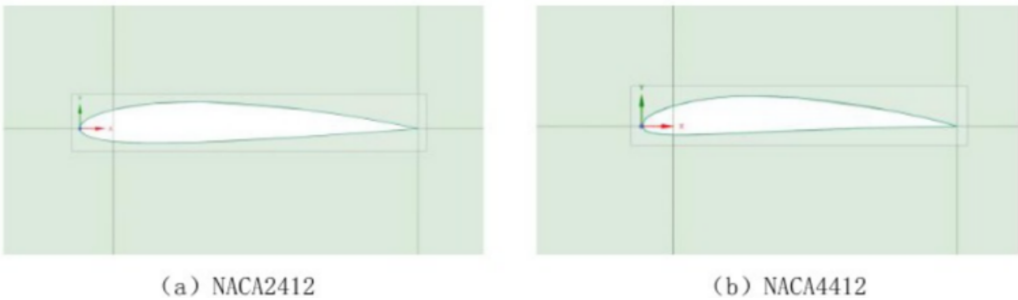

Figure 1. Geometric models of NACA2412 and NACA4412 (picture credit: original)

2.2. Mesh generation

Firstly, the fluid domain is meshed. Grid generation is an important part of numerical simulation, and the completion degree will directly affect the accuracy of the numerical results [4]. In this paper, the “C-type” computational domain and two-dimensional structured grid are selected for the grid generation of the computational domain and the airfoil. As shown in Fig. 2(a), the computational domain is divided into 6 sub-domains to better simulate the flow movement. The external domain is meshed with a cell size of 0.5m in length to optimize the calculation efficiency and save the

DOI: 10.54254/2755-2721/2025.MH25948

calculation time. The internal domain is meshed with a refined treatment by means of reverse bias pressure, using a fine grid of 10−4m to more accurately reflect the flow movement. By verifying with different grid densities, ensuring that the results are not affected, it is finally decided to use about 240 thousand grids for simulation. Finally, the far-field boundary conditions are set to the velocity inlet and pressure inlet.The grid is shown in Figure 2(b) and the local details around the airfoil are shown in Figures 2(c) and (d).

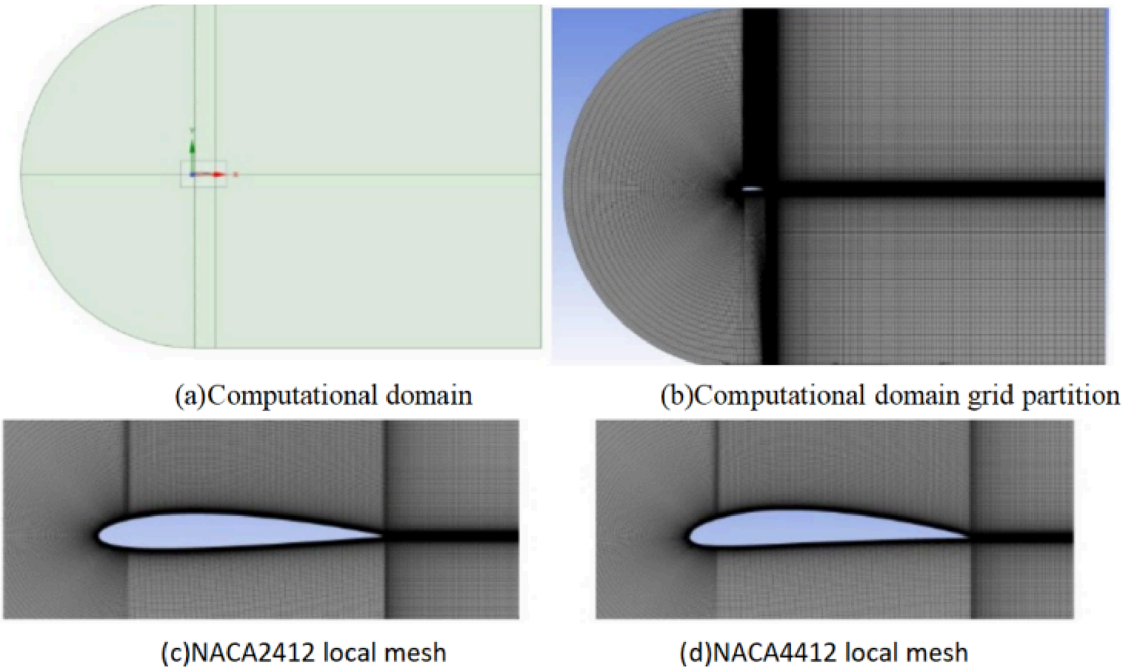

Figure 2. Computational domain grid and the local grid details of NACA2412 and NACA4412 (picture credit: original)

2.3. Flow control equations

In this paper, the CFD fluid simulation software is used, and the governing equations are the incompressible continuity equation and the Navier-Stokes equations [5].

The continuity equation is expressed as follows:

$$\frac{\partial \rho}{\partial t} + \frac{\partial \rho u}{\partial t} + \frac{\partial \rho v}{\partial t} + \frac{\partial \rho w}{\partial t} = 0 \tag{1}$$

where ρ is the density and u, v and w are the velocity components in the x,y and z directions, respectively. For an incompressible flow, ρ is constant. In a two-dimensional simulation, the z-directional velocity component w is zero [6].

Navier-stokes equation as follows [7]:

$$\frac{\partial \vec{V}}{\partial t} + \left(\vec{V} \bullet \nabla\right)\vec{V} = -\frac{1}{\rho}\nabla p + v\nabla^2\vec{V} + \vec{f} \tag{2}$$

The two terms on the left of the equation are the rate of change of the velocity field with time, and the convective term, in which the convective term plays a major role in this calculation. The

DOI: 10.54254/2755-2721/2025.MH25948

three terms on the right of the equation are the pressure term, the viscous term, and the body force term.

The model used for simulation calculation is k-omega SST two- equation turbulence model [8], the first equation is the turbulent kinetic energy equation, and the second equation is the specific dissipation rate equation.

The expression of turbulent kinetic energy equation is as follows:

$$\frac{\partial(\rho k)}{\partial t} + \nabla \bullet (\rho v k) = P_k - \beta^* \omega k + \nabla\left[\left(\mu + \sigma_k \mu_t\right)\nabla k\right] \tag{3}$$

where ρ is the density, t is time, k is the turbulent kinetic energy, Pk is the turbulent kinetic energy generation term, σ∗ is the turbulent Prandtl number, and β∗ is an empirical constant, taken as 0.09.

The expression of the energy dissipation rate equation is as follows:

$$\frac{\partial(\rho\omega)}{\partial t} + \nabla \bullet (\rho v \omega) = \alpha \frac{\omega}{k} P_k - \beta\rho\omega^2 + \nabla \bullet \left[\mu + \sigma_\omega \mu_t \nabla\omega\right] + 2\left(1 - F_1\right)\rho\sigma_{\omega 2}\frac{1}{\omega}\nabla k \nabla\omega \tag{4}$$

where ω is the specific dissipation rate, μt is the shear-stress transport SST-modified eddy viscosity, and α and β are model coefficients [9].

2.4. Boundary conditions

To obtain more accurate numerical results, the CFD simulation in this paper is set to 1000 iterations, and the residual is set to 10-6 to ensure that the results converge. The boundary conditions of simulation calculation are given in detail in Table 1.

Table 1. Boundary condition setting parameters

Solver	Pressure-based Solver
Area(m2)	1
Chord length(m)	1
Density(kg/m3)	1.225
Visicosty coefficient(kg/m-s)	17894e-5
Pressure(Pa)	0
Temperature(k)	288.16
Entry velocity(m/s)	33
Reynolds number	2.2×10^6
Momentum	Second-order upwind scheme
Pressure-velocity coupling	coupling
Specific heats	1.4

DOI: 10.54254/2755-2721/2025.MH25948

3. Results

3.1. Comparison and analysis of aerodynamic coefficients for different angle of attack ranges

3.1.1. Lift coefficient comparison

The lift coefficients of NACA2412 and NACA4412 are given in Table 2 and the variation of lift coefficient with the angle of attack for both airfoils is shown in Fig. 3(a). The lift coefficient is seen to vary with the angle of attack and the angle of attack at which the maximum lift coefficient is obtained for a given airfoil is the stall angle of that airfoil.

Figure 3(a) compares the lift coefficients of NACA2412 and NACA4412 airfoils at angles of attack from 0° to 18°. Both airfoils exhibit a linear increase in lift coefficient up to 10°. The lift lines of NACA2412 and NACA4412 have similar curvatures, but NACA4412 has a higher lift coefficient in this range. As the angle of attack increases, the lift coefficient rises, peaks at the stall angle, and then declines. The stall angle for NACA2412 is approximately 16°. The stalling angle of NACA4412 airfoil is close to 13°. From the slope of the two airfoils' post-stall curves, it can be seen that the stall curve of NACA2412 is gentler, and that of NACA4412 is steep. From Table 2, it can be seen that the maximum lift coefficient of NACA2412 is about 1.58, and that of NACA4412 is only 1.4 1. The maximum value of the lift coefficient of NACA241 2 is greater than that of NACA4412 [9].

Table 2. Lift coefficient comparison of NACA2412 and NACA4412

Attack angle(°)	NACA2412Cl	NACA2412Cl
0	0.20907813	0.20907813
2	0.42308866	0.42308866
4	0.63451036	0.63451036
6	0.84119224	0.84119224
8	1.03941140	1.03941140
10	1.22383440	1.22383440
12	1.38628281	1.38628281
13	1.43959111	1.43959111
14	1.51289950	1.51289950
15	1.55501758	1.55501758
16	1.57754751	1.57754751
17	1.57122422	1.57122422
18	1.54753783	1.54753783

DOI: 10.54254/2755-2721/2025.MH25948

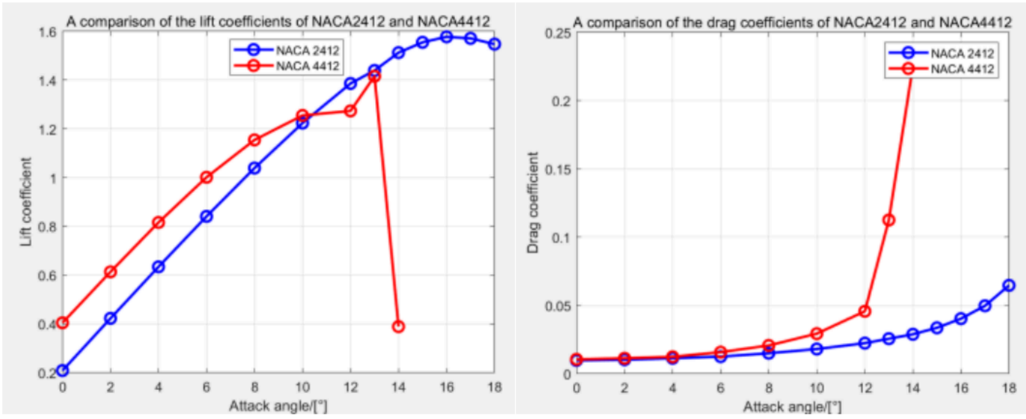

Figure 3. Lift coefficient and drag coefficient diagram of NACA2412 and NACA4412 (picture credit: original)

3.1.2. Drag coefficient comparison

Figure 3(b) shows a comparison of the drag coefficient of NACA241 2 andNACA4412 within the range of 0-16° of the angle of attack. The specific data are shown in Table 3. It can be seen from Fig. 3(b) that when the attack angle is below 8°, the drag coefficients ofthe two airfoils are very close, and NACA4 412 is slightly higher than NACA2412. As the attack angle increases to 12°, the drag coefficient of NACA4412 suddenly increases dramatically. From the chart, the minimum drag coefficient of NACA2412 is about 0.0098, and the minimum drag coefficient of NACA4412 is about 0. 0105. Overall, the NACA241 2 airfoil produces less drag in flight [10].

Table 3. A comparison of the drag coefficients of NACA2412 and NACA4412

Attack angle(°)	NACA2412Cd	NACA2412Cd
0	0.00976177	0.01054153
2	0.01028651	0.01136002
4	0.01134642	0.01240201
6	0.01255817	0.01584466
8	0.01501110	0.02072132
10	0.01812613	0.02937142
12	0.02242854	0.04575105
13	0.02567548	0.11258854
14	0.02892241	0.22527725
15	0.03364761	0.08321181
16	0.04034915	0.14430908
17	0.04978051	0.16962121
18	0.06470669	0.24328168

DOI: 10.54254/2755-2721/2025.MH25948

3.2. Cloud map analysis

3.2.1. Analysis of the pressure cloud map

Figure 4 illustrates the pressure distribution for NACA2412 and NACA4412 airfoils at angles of attack ranging from 0 to 18 degrees.

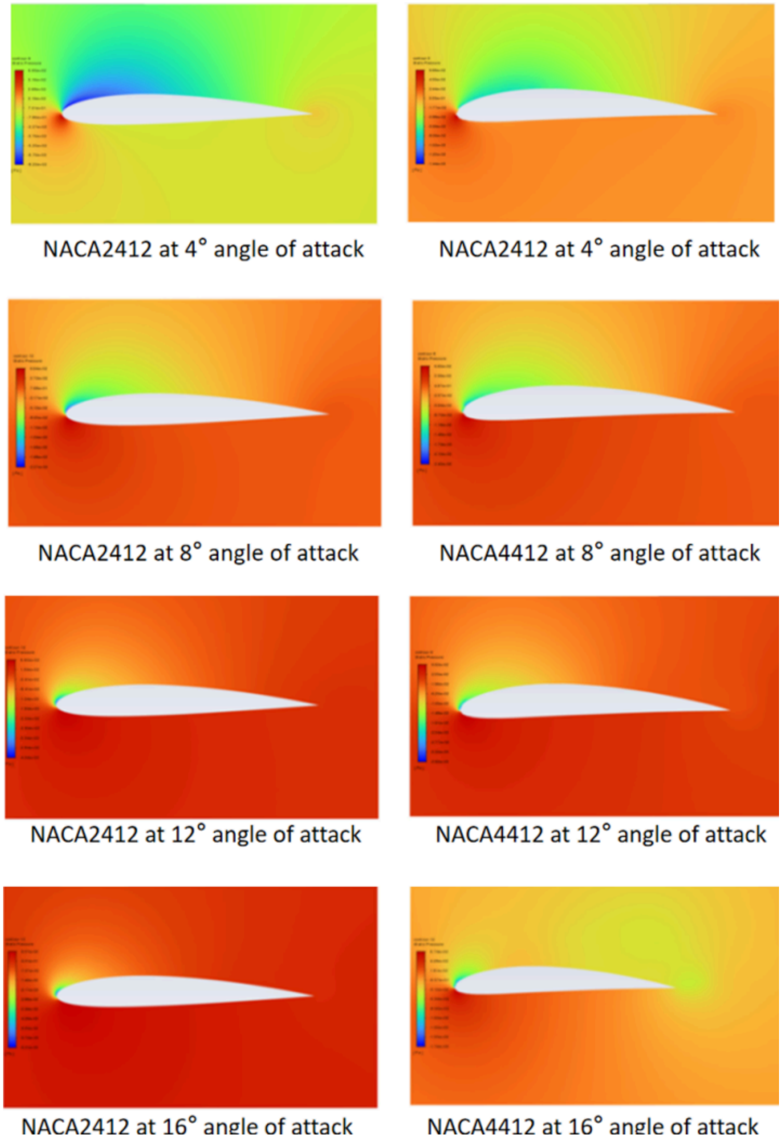

Figure 4. Pressure contours for NACA2412 and NACA4412 (picture credit: original)

As the angle of attack increases, the pressure center on the upper surface of both airfoils progressively shifts toward the leading edge. This behavior aligns with Bernoulli's principle, which states that the curved upper surface experiences faster flow and lower pressure compared to the lower surface, and when a certain pressure difference is generated between the upper and lower surfaces of the airfoil, the airflow can produce lift to effectively push the wing upward. In the range of small angle of attack of 0°-5°, the negative pressure area on the upper surface of NACA 2412 is gentle, and the positive pressure area on the lower surface is evenly distributed. While the negative pressure area on the upper surface of NACA4412 is larger, and the positive pressure on the lower

DOI: 10.54254/2755-2721/2025.MH25948

surface is higher. It shows that NACA4412 performs better in this range. With the increase of the angle of attack to the range of 8°-12°, the pressure centers of 2412 and 4412 both move forward, and a small area of low velocity appears at the rear. However, NACA44 12, with its larger camber, makes the pressure difference between the upper and lower surfaces greater than that of NACA2412. It is shown that NACA4412 performs better in this range. In the range of high angle of attack of 12°-16°, NACA2412 is still not obvious, but the pressure cloud map of NACA4412 is chaotic and has stalled, indicating that NACA2412 has a stall-delay characteristic in the range of high angle of attack.

3.2.2. Analysis of the velocity cloud chart

The velocity distribution for NACA2412 and NACA4412 airfoils at angles of attack between 0° and 18° is depicted in Figure 5.

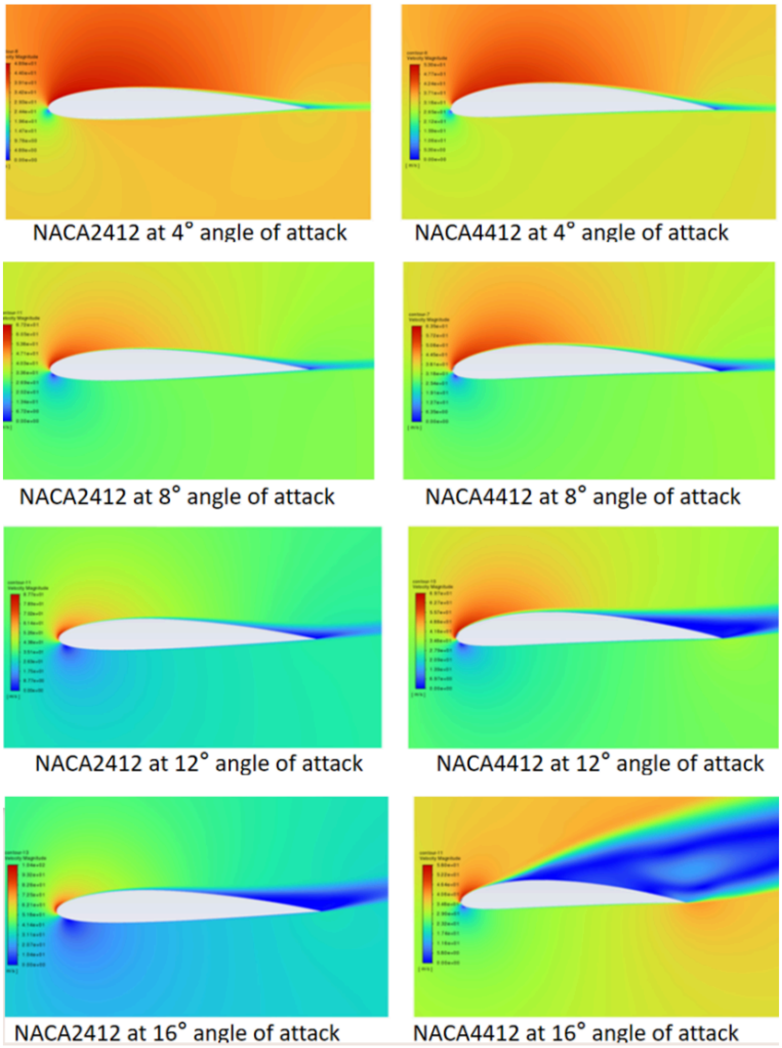

Figure 5. Velocity contours for NACA2412 and NACA4412 (picture credit: original)

Figure 5 illustrates that as the angle of attack increases, the low-velocity region at the trailing edge progressively moves toward the leading edge. and this phenomenon is reflected in both airfoils. In the range of small angle of attack of 0°-5°, the surface velocity of NACA2412 increases slowly, while the high velocity area of NACA4412 is wider, indicating that NACA4412 exhibits better lift

DOI: 10.54254/2755-2721/2025.MH25948

characteristics in this range. As the angle of attack increases to the range of 8° -12°, small low-velocity areas appear at the trailing edge of both NACA2412 and NACA4 412, but the high-velocity area on the surface of NACA4412 is wider, indicating that NACA4412 exhibits better aerodynamic characteristics in this range. When the angle of attack increases to the range of 12°-16°, the low-velocity area at the trailing edge of NACA2412 slowly moves forward to the leading edge, while a large area of low-velocity separation area appears on the surface of NACA4412. This indicates that in this range, NACA 2412 has a larger stall angle of attack and a gentler stall. The law of the contour map is in remote correspondence with the lift coefficient data in Table 2, further illustrating the accuracy of the simulation results.

4. Conclusion

In this paper, the aerodynamic characteristics of NACA2412 and NACA4412 airfoils are fully investigated and compared based on ANSYS Fluent. The two-dimensional flow characteristics were numerically simulated with K- w SST turbulence model and pressure-based solver, and the pressure, velocity distribution and aerodynamic characteristics of the two airfoils at different angles of attack are analyzed in detail. The results obtained in this paper are as follows: The stall angle of NACA2412 is 16 degrees, and that of NACA4412 is 13 degrees. At a high angle of attack, the flow over the NACA2412 gradually separates, and the stall is relatively gentle. The flow over the NACA4412 suddenly separates at stall, and the stall is severe. NACA2412 has stronger anti-stall ability and is safer to work at a moderate angle of attack.

(1)The NACA4412 airfoil, with its larger camber, is advantageous for low-speed, low-angle-of-attack flight, providing higher lift at low speeds. Therefore, the NACA44 12 is more advantageous for low-speed, high-lift aircraft. The NACA2 412, with its superior lift-to-drag ratio and higher stall angle of attack, may be a better choice for aircraft operating at moderate angles of attack or requiring high maneuverability.

(2)Future research can combine wind tunnel experiments to further verify the CFD results and explore the influence of aerodynamic characteristics of the three-dimensional aspect ratio effect to further verify the accuracy of the experimental results.

(3)Future research should focus on multi-disciplinary cross-collaboration, promoting airfoil aerodynamic characteristics research into a new stage. Currently, the primary methods for assessing the aerodynamic performance of wind turbine airfoils are wind tunnel tests and numerical simulations. Wind tunnel testing is time-consuming and expensive. With advancements in computer technology and improvements in turbulence models, numerical simulation has become the predominant method for researching wind turbine airfoil aerodynamics. Using Ansys to study airfoil performance can optimize wind turbine airfoils and enhance wind energy conversion efficiency. Moreover, the study of airfoil aerodynamic performance can also design the wave energy conversion device to optimize the energy capture.

References

[1] Li, F., Li, Z., Han, H.: Overall Design of a Submarine Launched Unmanned Aerial Vehiclecapture. S. 2023 Asia-Pacific International Symposium on Aerospace Technology (APISAT 2023) Proceedings. APISAT 2023.

[2] Pritam S., Harshpreet S.: Numerical Analysis of Aerodynamic Performance Characteristics of NACA 2312 and NACA 2412. International Journal of Innovative and Research Technology, 2020, 5(3), 1.

[3] Li Z., Guo H., Yuan W., et al. PIV Testing and Numerical Analysis of Flow Around High Angle-of-Attack Airfoils. Test Technology Group of the Ship Mechanics Academic Committee of China Shipbuilding Society. Proceedings of

DOI: 10.54254/2755-2721/2025.MH25948

the 2021 Academic Conference of the Test Technology Group of the Ship Mechanics Academic Committee of China Shipbuilding Society. Ningbo University; 2021: 227-236.

[4] Zhang, C.: Study on Heat Transfer Enhancement of Flat Plate Solar Water Heater with Sudden Expansion by Turbulence Generators. Lanzhou Jiaotong University, 2023.

[5] Wang, Z.: Analysis of Aerodynamic Performance of Typical Airfoils and Safety of Aerospace Materials. Nanchang Hangkong University, 2020.

[6] Zou Z., Li B.: Simulation and Analysis of Aerodynamic Performance of NACA2412 Wing. China Water Transport, 2021, 21(20): 53-54+57.

[7] Zuo, L., Si, H., Li, Y., et al.: CFD Discretization Error Analysis Based on Richardson Extrapolation Method. Command Control & Simulation, 2022, 44(01): 58-62.

[8] Wang, J.: Transonic static aeroelastic and longitudinal aerodynamic characteristics of a low-aspect-ratio swept wing, AIP Advances, 2019

[9] Vivekanandan, A., Ramesh, K.: Photoelastic analysis of crack terminating at an arbitrary angle to the bimaterial interface under four point bending, Theoretical and Applied Fracture Mechanics, 2023, 127, 104075

[10] Xu, S., Wu, J., Yang, X., Zhang, S.: Trajectory tracking and hydrodynamics of a tethered underwater vehicle based on hybrid grid, Ocean Engineering, 2021, 241, 110051